

---

---

SPECTROSCOPY  
OF CONDENSED MATTER

---

---

# Optical Spectroscopy of Kramers Doublets of an $\text{Er}^{3+}$ Ion in a Two-Dimensional Frustrated Magnetic $\text{Cu}_3\text{Er}(\text{SeO}_3)_2\text{O}_2\text{Cl}$

S. A. Klimin<sup>a,\*</sup>, P. S. Berdonosov<sup>b</sup>, and E. S. Kuznetsova<sup>b</sup>

<sup>a</sup> Institute for Spectroscopy, Russian Academy of Sciences, Troitsk, Moscow, 108840 Russia

<sup>b</sup> Department of Chemistry, Lomonosov Moscow State University, Moscow, 119991 Russia

\*e-mail: klimin@isan.troitsk.ru

Received September 19, 2020; revised September 21, 2020; accepted October 5, 2020

**Abstract**—Francisites,  $\text{Cu}_3\text{M}(\text{YO}_3)_2\text{O}_2\text{X}$  ( $\text{M} = \text{Bi}$  or rare earth,  $\text{Y} = \text{Se, Te}$ ,  $\text{X} = \text{Br, Cl, or I}$ ), attract close attention from researchers because of their interesting magnetic properties, such as metamagnetic transitions in relatively weak magnetic fields and magnetic phase transitions with spin reorientation; they also can serve as model systems for the study of two-dimensional and frustrated magnetism. In this work, we have performed a low-temperature optical spectroscopic study of erbium francisite,  $\text{Cu}_3\text{Er}(\text{SeO}_3)_2\text{O}_2\text{Cl}$ . The observed splitting of spectral lines corresponding to  $f$ - $f$  transitions in the  $\text{Er}^{3+}$  Kramers ion unambiguously indicates the magnetic ordering of the crystal at a temperature of  $T_N = 37.5$  K. The temperature dependence of the splitting of the ground doublet of the erbium ion is determined. The contributions of erbium to the heat capacity and to the magnetic susceptibility of  $\text{Cu}_3\text{Er}(\text{SeO}_3)_2\text{O}_2\text{Cl}$  are calculated.

**Keywords:** erbium francisite, magnetic ordering, transmission spectra, splitting of Kramers doublets

**DOI:** 10.1134/S0030400X21010094

## INTRODUCTION

Low-dimensional and frustrated magnetic systems are of great interest for the physics of magnetism [1]. Various non-classical magnetic states are realized in them, including spin liquids, skyrmions, vortices, etc. [2–6]. Francisites,  $\text{Cu}_3\text{M}(\text{YO}_3)_2\text{O}_2\text{X}$  ( $\text{M} = \text{Bi}$  or rare earth,  $\text{Y} = \text{Se, Te}$ ,  $\text{X} = \text{Br, Cl, or I}$ ), have been recognized as interesting systems to study two-dimensional and frustrated magnetism. A synthetic analog of the francisite mineral,  $\text{Cu}_3\text{Bi}(\text{SeO}_3)_2\text{O}_2\text{Cl}$  (with chlorine being replaced by bromine and with a six-sublattice noncollinear antiferromagnetic system and Néel temperature of  $T_N = 27.4$  K), has been recognized to be a model system in which the Thouless–Kosterlitz transition can occur [7]. Later, a structural phase transition was revealed in the  $\text{Cu}_3\text{Bi}(\text{SeO}_3)_2\text{O}_2\text{Cl}$  mineral itself with an antiferroelectric distortion of the lattice. Bismuth-containing francisites of various compositions in Y and X turned out to be objects of close attention for studies of their magnetic and ferroelectric properties [7–11].

The francisite mineral crystallizes in the orthorhombic space group  $Pmmn$  [12–15]. The main feature of the crystal structure is the occurrence of two-dimensional layers of copper (Fig. 1), with copper atoms inside the layer forming a corrugated kagome lattice with frustrated magnetic interactions. Rare-earth ions that replace bismuth are located in eight

oxygen ion coordinated polyhedra, and their crystallographic position has the  $C_{2v}$  symmetry. The first francisite crystal in which bismuth was replaced by a rare earth element was  $\text{Cu}_3\text{Er}(\text{SeO}_3)_2\text{O}_2\text{Cl}$ , which is isostructural to the original mineral [16]. Later, about 25 rare earth compounds from the francisite family were synthesized at the Department of Chemistry of the Lomonosov Moscow State University [17, 18].

Rare-earth francisites are being thoroughly investigated by various methods [19–25]. They, similarly to bismuth francisites, are ordered into an antiferromagnetic phase at low temperatures. The Néel temperature in them is higher than in  $\text{Cu}_3\text{Bi}(\text{SeO}_3)_2\text{O}_2\text{Cl}$  (34–38 K). Magnetic rare-earth ions form an additional magnetic sublattice, which can actively affect realized magnetic structures. Spectroscopic studies made it possible to conclude that, in the case of a strong single-ion magnetic anisotropy of a rare-earth ion, spin-reorientation phase transitions can occur, which are most pronounced in the case of samarium francisite [21] and ytterbium francisite [22].

In this work, by using the method of spectroscopy of Kramers doublets of the  $\text{Er}^{3+}$  ion, we studied erbium francisite,  $\text{Cu}_3\text{Er}(\text{SeO}_3)_2\text{O}_2\text{Cl}$ , to extract information on the magnetic ordering and magnetic properties of the crystal under study at low temperatures.

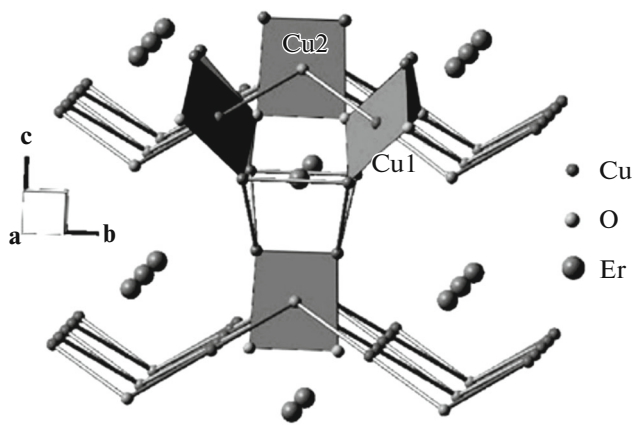


**Fig. 1.** Fragment of the crystal structure of erbium francisite,  $\text{Cu}_3\text{Er}(\text{SeO}_3)_2\text{O}_2\text{Cl}$ . The corrugated two-dimensional copper layers are parallel to the  $ab$  crystallographic plane. Erbium ions are located between the layers.

## EXPERIMENTAL TECHNIQUES

Polycrystalline samples of  $\text{Cu}_3\text{Er}(\text{SeO}_3)_2\text{O}_2\text{Cl}$  were prepared by solid-phase synthesis at the Department of Chemistry, Moscow State University. The results of the X-ray study showed that the sample has a  $Pm\bar{m}n$  structure and does not contain other phases. A detailed description of the synthesis procedure can be found in [17]. To study the transmission spectra, we used the standard technique for preparing tablets with potassium bromide filling. To prepare the sample, polycrystalline powder of  $\text{Cu}_3\text{Er}(\text{SeO}_3)_2\text{O}_2\text{Cl}$  was taken in an amount of  $\sim 12$  mg, was then thoroughly stirred with  $\sim 300$  mg of optically pure KBr. Then, the resulting mixture was ground in an agate mortar, placed in a mold, and pressed into a tablet of 13 mm in diameter at a pressure of  $\sim 5$  at.

Transmission spectra were measured on a Bruker IFS125 Fourier spectrometer using a liquid nitrogen cooled InSb detector and a  $\text{CaF}_2$  beam splitter. In low-temperature measurements, the sample was placed in an indium envelope with a through hole 5 mm in diameter. Indium was mechanically pressed against the cold finger of a CryoMech ST403 closed-cycle optical helium cryostat. The sample was kept in vacuum better than  $5 \times 10^{-4}$  Torr. Evacuation was performed using a Varian V70 Turbo turbomolecular pump. Temperature was controlled with an accuracy of 0.1 K using a Scientific Instruments controller.

## EXPERIMENTAL RESULTS

Figure 2 shows the transmission spectra of  $\text{Cu}_3\text{Er}(\text{SeO}_3)_2\text{O}_2\text{Cl}$  in the range of the  ${}^4I_{15/2} \rightarrow {}^4I_{13/2}$  transition from the ground multiplet of the  $\text{Er}^{3+}$  ion to the first excited multiplet at different temperatures. The three lowest in frequency transition spectral lines are shown. At a temperature of  $T_N = 37.5$  K, a sharp

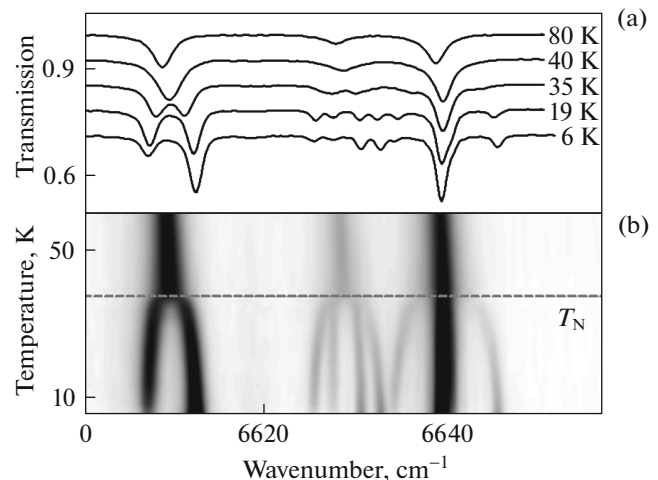


**Fig. 2.** The three lowest in frequency spectral lines of the transition from the ground  ${}^4I_{15/2}$  multiplet to the excited  ${}^4I_{13/2}$  multiplet in the  $\text{Er}^{3+}$  ion in  $\text{Cu}_3\text{Er}(\text{SeO}_3)_2\text{O}_2\text{Cl}$ . (a) Transmission spectra at different temperatures and (b) intensity map.

splitting of the spectral lines occurs, which indicates magnetic ordering. According to the consequence from the Kramers theorem, only a magnetic field can remove Kramers degeneracy, in this case, this is the internal effective magnetic field (exchange field).

The intensity map presented in Fig. 2b shows that the three lines split into a different number of components: two, four, and three. This is because the splitting scheme is specific, namely, the splitting values for the upper and lower levels involved in a given spectral transition are different (Fig. 3). For the transition that corresponds to the spectral line at  $6610 \text{ cm}^{-1}$ , the splitting of the upper doublet is zero; therefore, only two components are seen in the spectrum of the antiferromagnetic phase ( $T < T_N$ ). For the transition corresponding to the line at  $6624 \text{ cm}^{-1}$ , the splitting of the upper doublet is smaller than that of the lower doublet, and all the four components are observed. Finally, for the transition that corresponds to the line at  $6640 \text{ cm}^{-1}$ , the splittings of the upper and the lower doublets are the same. As a result, the two components coincide, and three lines are observed in the spectrum of the antiferromagnetic phase.

The splitting  $\Delta$  of the Kramers doublets is described by the following relation:

$$\Delta = \mu_B \sqrt{\sum_j (g_j B_j)^2}, \quad (1)$$

where  $\mu_B$  is the Bohr magneton, while  $g_j$  and  $B_j$  are the  $j$ th components ( $j = x, y, z$ ) of the magnetic  $g$  factors and the effective magnetic field that acts on the rare-earth ion inside the crystal. We note that, first, relation (1) underlines the anisotropic magnetic prop-

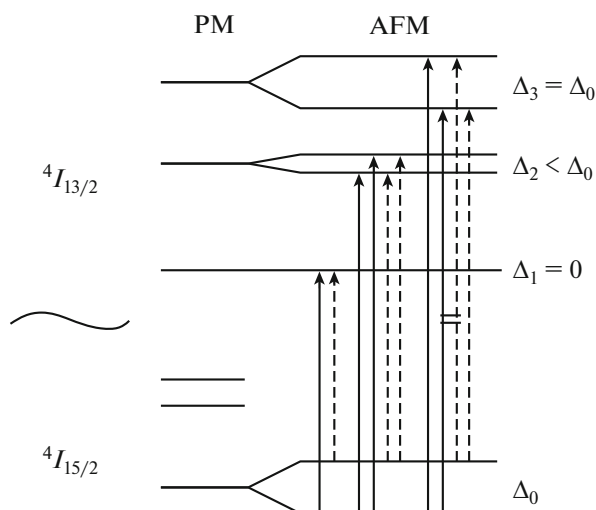


**Fig. 3.** Energy level diagram of the  $\text{Er}^{3+}$  ion in the paramagnetic (PM) and antiferromagnetic (AFM) phases. In the AFM phase, the Kramers doublets are split. Different cases of the relation between the splittings of the lower and upper doublets involved in the transition are realized.

erties of the rare-earth ion: in the case of zero values of some components of the magnetic  $g$  factor, the effective field of only along a certain direction can split this Kramers doublet. In certain cases, this makes it possible to use a rare earth ion as a spectroscopic probe to indicate the direction of the crystalline magnetic field inside the crystal [26, 27]. Second, we understand that, as a result of the splitting of the ground doublet  $\Delta_0$ , in accordance with relation (1), the system receives an energy gain. If this gain is large enough, it will be profitable for the system to obtain this gain if it is associated with the rotation of the field  $B$ . Precisely this is the nature of spin-reorientation transitions, which are realized, e.g., in the case of samarium francisite [21] and ytterbium francisite [24]. We emphasize that, for the erbium francisite,  $\text{Cu}_3\text{Er}(\text{SeO}_3)_2\text{O}_2\text{Cl}$ , studied in this work, the ground doublet of the rare-earth ion is noticeably split along with the ordering of the copper subsystem. It can be inferred from this that the anisotropy of the magnetic  $f$  subsystem in  $\text{Cu}_3\text{Er}(\text{SeO}_3)_2\text{O}_2\text{Cl}$  either has the same character as the anisotropy of the magnetic subsystem of copper, or dominates.

Figures 4a and 4b show the temperature dependences of the frequency and half-width of the spectral line at  $6610\text{ cm}^{-1}$  and its split components. These plots allow one to determine the temperature of magnetic ordering ( $T_N = 37.5\text{ K}$ ) and to extract the temperature dependence of the splitting of the ground doublet  $\Delta_0$  (shown in Fig. 4c).

Applying the approach that we developed and that we outlined in [28, 29] and using the dependence  $\Delta_0(T)$  obtained in this work, we were also able to calculate the temperature dependences for the magnetic

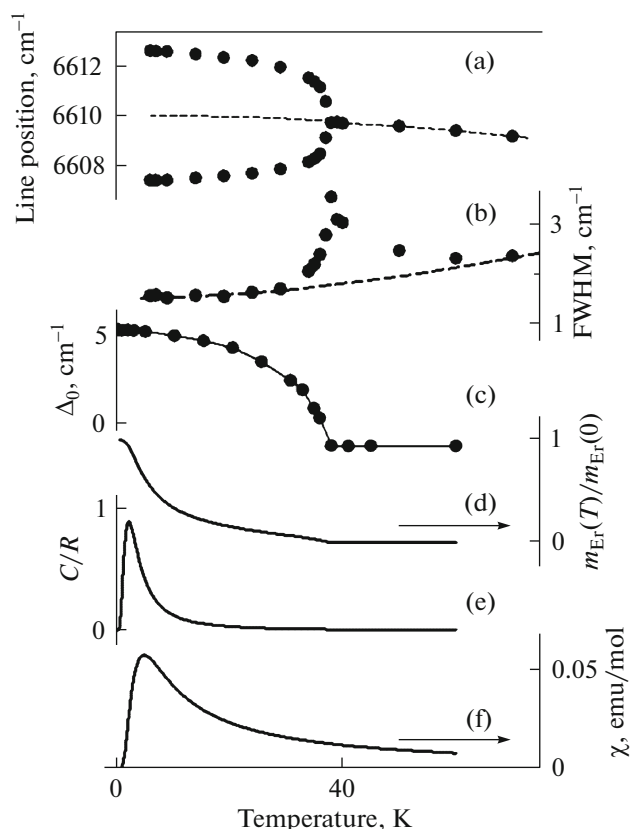


**Fig. 4.** Temperature dependences of (a) the frequencies of maxima of observed peaks for the line at  $6610\text{ cm}^{-1}$ , (b) the half-widths of the peaks of the same spectral line, (c) the splitting of the ground doublet  $\Delta_0$  of the  $\text{Er}^{3+}$  ion, (d) the normalized magnetic moment  $m_{\text{Er}}$  of the  $\text{Er}^{3+}$  ion, and the contributions of the  $\text{Er}^{3+}$  ion to the (e) specific heat capacity  $C$  and (f) the magnetic susceptibility of  $\text{Cu}_3\text{Er}(\text{SeO}_3)_2\text{O}_2\text{Cl}$ .

moment of the  $\text{Er}^{3+}$  ion in  $\text{Cu}_3\text{Er}(\text{SeO}_3)_2\text{O}_2\text{Cl}$  (Fig. 4d) and the contributions of erbium (Schottky anomaly) to the specific heat capacity  $C(T)$  (Fig. 4e) and the magnetic susceptibility (Fig. 4f).

## CONCLUSIONS

We measured the transmission spectra and their temperature dependences (down to helium temperatures) of erbium francisite,  $\text{Cu}_3\text{Er}(\text{SeO}_3)_2\text{O}_2\text{Cl}$ , in the range of the  ${}^4I_{15/2} \rightarrow {}^4I_{13/2}$  spectral transition in the  $\text{Er}^{3+}$  ion. The splitting of spectral lines (at  $T_N = 37.5\text{ K}$ ) unambiguously indicates the appearance of an effective magnetic field associated with the antiferromagnetic ordering of the crystal, which splits the Kramers doublets of the  $\text{Er}^{3+}$  ion. The single-ion magnetic anisotropy of the magnetic  $f$  subsystem either coincides with the anisotropy of the  $d$  subsystem or dominates. The temperature dependence of the splitting of

the ground doublet of the erbium ion was determined. It was used to calculate the Schottky anomalies in the heat capacity and the magnetic susceptibility.

#### FUNDING

This work was financially supported by the Russian Foundation for Basic Research, project no. 19-02-00251.

#### CONFLICT OF INTEREST

The authors declare that they have no conflict of interest.

#### REFERENCES

1. A. Vasiliev, O. Volkova, E. Zvereva, and M. Markina, *NPJ Quantum Mater.* **3**, 18 (2018).
2. S. M. Yan, D. A. Huse, and S. R. White, *Science* (Washington, DC, U. S.) **332**, 1173 (2011).
3. X. G. Wen, *Phys. Rev. B* **65**, 165113 (2002).
4. S. Muehlbauer, B. Binz, F. Jonietz, C. Pfleiderer, C. Rosch, A. Neubauer, R. Georgii, and P. Boeni, *Science* (Washington, DC, U. S.) **323**, 915 (2009).
5. C. Nayak and K. Shtengel, *Phys. Rev. B* **64**, 064422 (2001).
6. D. Grohol, K. Matan, J. H. Cho, S. H. Lee, J. W. Lynn, D. G. Nocera, and Y. S. Lee, *Nat. Mater.* **4**, 323 (2005).
7. M. Pregelj, O. Zaharko, A. Gunther, A. Loidl, V. Tsurkan, and S. Guerrero, *Phys. Rev. B* **86**, 144409 (2012).
8. H. C. Wu, W. J. Tseng, P. Y. Yang, K. D. Chandrasekhar, H. Berger, and H. D. Yang, *J. Phys. D: Appl. Phys.* **50**, 265002 (2017).
9. D. A. Prishchenko, A. A. Tsirlin, V. Tsurkan, A. Loidl, A. Jesche, and V. G. Mazurenko, *Phys. Rev. B* **95**, 064102 (2017).
10. E. Constable, S. Raymond, S. Petit, E. Ressoushe, F. Bourdarot, J. Debray, M. Josse, O. Fabelo, H. Berger, S. de Brion, and V. Simonet, *Phys. Rev. B* **96**, 014413 (2017).
11. V. Gnezdilov, Yu. Pashkevich, P. Lemmens, V. Kurnosov, P. Berdonosov, V. Dolgikh, E. Kuznetsova, V. Pryadun, K. Zakharov, and A. Vasiliev, *Phys. Rev. B* **96**, 115144 (2017).
12. A. Pring, B. M. Gatehouse, and W. D. Birch, *Am. Mineral.* **75**, 1421 (1990).
13. J. A. Mandarino, *Eur. J. Mineral.* **6**, 337 (1994).
14. S. V. Krivovichev, G. L. Starova, and S. K. Filatov, *Miner. Mag.* **63**, 263 (1999).
15. E. V. Nazarchuk, S. V. Krivovichev, O. Y. Pankratova, and S. K. Filatov, *Phys. Chem. Miner.* **27**, 440 (2000).
16. R. Berrigan and B. M. Gatehouse, *Acta Crystallogr., C* **52**, 496 (1996).
17. P. S. Berdonosov and V. A. Dolgikh, *Russ. J. Inorg. Chem.* **53**, 1353 (2008).
18. P. S. Berdonosov, E. S. Kuznetsova, and V. A. Dolgikh, *Crystals* **8**, 159 (2018).
19. K. V. Zakharov, E. A. Zvereva, P. S. Berdonosov, E. S. Kuznetsova, V. A. Dolgikh, L. Clark, C. Black, P. Lightfoot, W. Kockelmann, Z. V. Pchelkina, S. V. Streltsov, O. S. Volkova, and A. N. Vasiliev, *Phys. Rev. B* **90**, 214417 (2014).
20. K. V. Zakharov, E. A. Zvereva, E. S. Kuznetsova, P. S. Berdonosov, V. A. Dolgikh, M. M. Markina, A. V. Olenev, A. A. Shakin, O. S. Volkova, and A. N. Vasiliev, *J. Alloys Compd.* **685**, 442 (2016).
21. K. V. Zakharov, E. A. Zvereva, M. M. Markina, M. I. Stratan, E. S. Kuznetsova, S. F. Dunaev, P. S. Berdonosov, V. A. Dolgikh, A. V. Olenev, S. A. Klimin, L. S. Mazaev, M. A. Kashchenko, M. A. Ahmed, A. Banerjee, S. Bandyopadhyay, et al., *Phys. Rev. B* **94**, 054401 (2016).
22. S. A. Klimin and I. V. Budkin, *EPJ Web of Conf.* **132**, 02010 (2017).
23. M. M. Markina, K. V. Zakharov, E. A. Zvereva, R. S. Denisov, P. S. Berdonosov, V. A. Dolgikh, E. S. Kuznetsova, A. V. Olenev, and A. N. Vasiliev, *Phys. Chem. Miner.* **44**, 277 (2017).
24. M. M. Markina, K. V. Zakharov, E. A. Ovchenkov, P. S. Berdonosov, V. A. Dolgikh, E. S. Kuznetsova, A. V. Olenev, S. A. Klimin, M. A. Kashchenko, I. V. Budkin, I. V. Yatsyk, A. A. Demidov, E. A. Zvereva, and A. N. Vasiliev, *Phys. Rev. B* **96**, 134422 (2017).
25. M. M. Markina, K. V. Zakharov, P. S. Berdonosov, V. A. Dolgikh, E. S. Kuznetsova, S. A. Klimin, O. B. Yumashev, and A. N. Vasiliev, *J. Magn. Magn. Mater.* **452**, 165721 (2019).
26. S. A. Klimin, A. S. Galkin, and M. N. Popova, *Phys. Lett. A* **376**, 1861 (2012).
27. M. N. Popova, S. A. Klimin, R. Troć, and Z. Bukowski, *Solid State Commun.* **102**, 71 (1997).
28. S. A. Klimin, A. S. Galkin, and M. N. Popova, *J. Alloys Compd.* **625**, 193 (2014).
29. E. A. Popova, S. A. Klimin, M. N. Popova, R. Klingeler, N. Tristan, B. Buchner, and A. N. Vasiliev, *J. Magn. Magn. Mater.* **331**, 133 (2013).

*Translated by V. Rogovoi*